THE PORE-WATER GEOCHEMISTRY OF THE Cu-Zn MINE TAILINGS AT KIDD CREEK, NEAR TIMMINS, ONTARIO, CANADA[1]

Tom A. Al[2], David W. Blowes[2], and John L. Jambor[3]

Abstract: The Kidd Creek Cu-Zn sulfide deposit near Timmins, ON. has been in operation since 1966, with current production of approximately 10,000 tpd. Tailings from the deposit contain 10 to 25 wt % pyrite and are disposed of as a thickened slurry in a 12- to 15-m high cone-shaped deposit in a 1,200-ha impoundment. Approximately 2.5 wt % natrojarosite residue from the zinc concentrate refining circuit has been disposed of with the tailings since 1985. The natrojarosite residue is limited to the upper 4.5 m of tailings. Three geochemical zones are defined by the pore-water concentrations of metals and SO_4. In the deepest zone, concentrations of most metals and anions are below detection and Na, K, Mg, Mn, Fe, Zn, HCO_3, and SO_4 are low, reflecting the mill discharge-water released with the tailings. In this zone, gypsum precipitation controls the concentrations of Ca and SO_4, the dominant elements in the pore water. Higher concentrations of Na, K, Mg, Mn, Fe, Zn, Pb, As, HCO_3, and SO_4 occur in an intermediate zone coincident with detectable natrojarosite in core samples. These increases indicate that some natrojarosite deposited with the tailings has dissolved. Higher Zn concentrations in the intermediate zone than in the deep zone are attributed to minor substitution of Zn in natrojarosite and to residual aqueous Zn-sulfate in the natrojarosite residue that is co-disposed with the tailings. A surficial zone with visible signs of sulfide oxidation contains high concentrations of Na, K, Mg, Mn, Fe, Zn, Pb, Cu, Ni, Co, Cd, Al, As, NO_3, and SO_4. Oxidation reactions, and the consequent pH decrease, have increased the concentrations of metals and SO_4 in the shallow pore-water.

Additional Key Words: mine tailings, tailings geochemistry, sulfide oxidation, jarosite, jarosite disposal, Kidd Creek.

Introduction

The Kidd Creek Cu-Zn deposit is approximately 25 km north of Timmins, ON, (fig. 1). The ore consists mainly of chalcopyrite, sphalerite, galena, and pyrite in massive ore, and chalcopyrite in stringers. In production since 1966, peak production of 12,400 tpd in 1985 has declined to approximately 10,000 tpd. Tailings are deposited as a thickened slurry in a 12- to 15-m high conical pile within a 1200-ha impoundment (Robinsky et al. 1991). The tailings consist of 10 to 25 wt % pyrite, 1 to 2 wt % pyrrhotite, 1 to 2 wt % combined sphalerite and chalcopyrite, 75 to 85 wt % gangue minerals, dominated by quartz and various silicates, 1 to 5 wt % carbonate minerals, and traces of numerous other minerals.

---

[1] Paper presented at the International Land Reclamation and Mine Drainage Conference and the Third International Conference on the Abatement of Acidic Drainage, Pittsburgh, PA, April 24-29, 1994.

[2] Waterloo Centre for Groundwater Research, University of Waterloo, Waterloo, Ont., Canada, N2L 3G1

[3] Mineral Sciences Laboratories, CANMET, Energy Mines and Resources Canada, 555 Booth St., Ottawa, Ont., Canada, K1A 0G1: Current Address: Waterloo Centre for Groundwater Research, University of Waterloo, Waterloo, Ont., Canada, N2L 3G1

Proceedings America Society of Mining and Reclamation, 1994 pp 208-217
DOI: 10.21000/JASMR94020208

https://doi.org/10.21000/JASMR94020208

The zinc-refining process used at Kidd Creek removes dissolved Fe from acidic Zn- and Fe-SO_4 solutions by precipitating natrojarosite ($NaFe_3(SO_4)_2(OH)_6$) (Scott and Dienstbach 1990). This natrojarosite residue was deposited in a settling pond until the pond reached capacity in 1985; since then the residue has been blended with the mill tailings prior to disposal. The natrojarosite residue, which averages 2.5 wt % of the tailings solids, is confined to the upper 1- to 4.5-m of the tailings impoundment.

In this study, pore-water geochemical data were collected through the vadose and saturated zones at several locations in the Kidd Creek impoundment (fig. 1). Coincident core samples of the tailings were collected for mineralogical analysis to identify the solid phases in contact with the pore water. These data and geochemical modeling were used to assess and interpret the geochemical mechanisms controlling the composition of the tailings pore water.

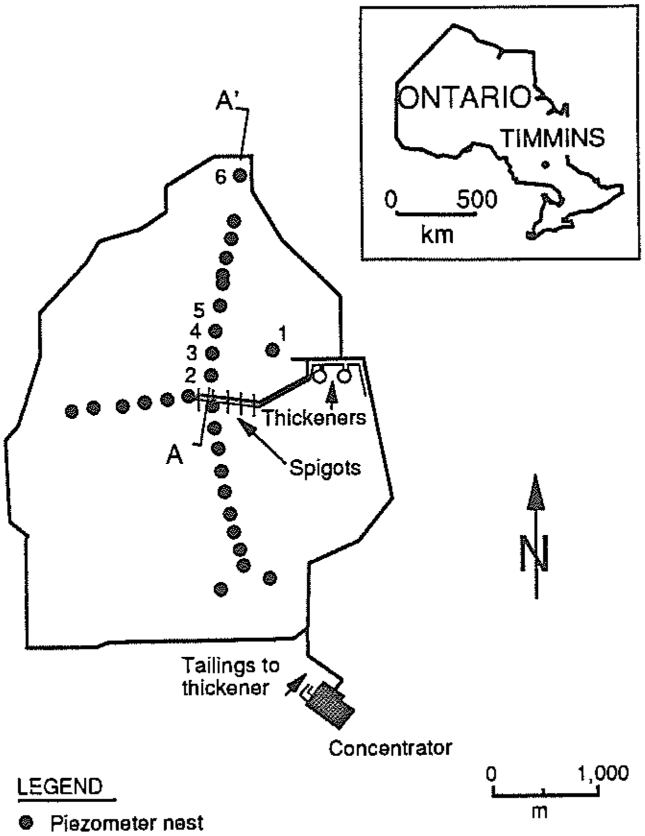

Figure 1. Location of the study area and piezometer nest sites.

Methods of Investigation

Pore water from the vadose zone at all sites (fig. 1) was sampled by collecting cores in thin-walled aluminum casing, 7.62-cm in diameter. The cores were cut into lengths of 20- to 25-cm, and pore water was squeezed from each section. Pore water from the saturated zone was collected with a peristaltic pump, in polyethylene lines, from polyethylene-lined stainless steel or PVC, single-completion drive-point piezometers installed at regular intervals between the water table and the base of the tailings. All piezometers were bailed dry prior to sampling. Groundwater temperatures were measured with a thermistor probe in the piezometer tip after the sample was collected. Determinations of pH and E_H of the vadose-zone pore-water were made at least three times during the collection of each sample. Measurements of pH and E_H of the saturated-zone pore-water were made in a sealed flow-through cell, maintained at the groundwater temperature. The Ross combination pH electrode was calibrated with standard buffers at pH 4 and 7, and the platinum redox electrode was checked regularly with Zobell's solution (Garrels 1960). All samples were filtered through 0.45-µm cellulose acetate filters, then split into two volumes. One was acidified with 12N, analytical-grade HCl to a pH of less than 1 for cation analysis, and the unacidified subsample was used for anion analysis. All samples were refrigerated until analysis. Cations were determined by atomic absorption spectroscopy, and anions by ion chromatography. Pore-water alkalinity was measured in the field on subsamples of 3- to 10-mL for vadose zone samples and 25- to 100-mL for saturated-zone samples using methyl red, bromcresol green indicator and a digital titrator or potentiometric titrations.

Results and Discussion

Pore-water data from two piezometer-nest sites (1 and 3 on fig. 1) are used to illustrate the pore-water geochemical evolution that followed tailings disposal. Limited tailings deposition has occurred at site 1 for the past 5 to 7 years. This site was chosen because the tailings near the surface display the most advanced oxidation observed within the impoundment. The maximum depth of sulfide oxidation at site 1 is only 20- to 40-cm. Site 3 is closer to the discharge road, and nearly continuous deposition has limited the extent of sulfide oxidation. Profiles of concentrations of dissolved constituents at sample sites along cross section A-A' (fig. 1) are shown in figure 2. Three zones of distinct pore-water chemical composition can be outlined from the data: a deep, mill discharge-water like zone, an intermediate zone with increased concentrations of Fe, Na, K, Pb, Zn, As, and SO_4 resulting from natrojarosite dissolution, and a surficial zone with high concentrations of metals and SO_4 due to sulfide oxidation. The components from natrojarosite dissolution have been transported by groundwater from the deepest level of natrojarosite detection at the upper dashed line, to the depth where ion concentrations decrease significantly (lower dashed line in figure 2).

Table 1. Mill discharge-water composition.

	1991	1992	Average
Cations, mg/L			
Ca	654	684	669
Mg	10.5	12.7	11.6
Mn	0.95	3.08	2.11
Na	47.3	50.3	48.8
K	25.7	20.4	23.1
Al	<0.02	<0.02	<0.02
Fe	0.05	<0.05	<0.05
Zn	0.55	9.06	4.81
Cu	0.07	0.31	0.19
Ni	0.07	0.15	0.11
Co	0.05	0.10	0.08
Cd	1.23	0.16	0.70
As, µg/L	<3.0	3.5	1.8
Anions, mg/L			
SO_4	1520	1780	1650
Cl	24.4	24.6	24.5
HCO_3	15.0	50.4	32.7

Notes. - Samples collected from the tailings thickener overflow. Natrojarosite is added to the tailings prior to thickening.

Mill Discharge-Water Zone

Nearly continuous accumulation of tailings at site 3 has minimized the effects of sulfide oxidation by atmospheric oxygen. Consequently, observed changes to the pore-water chemistry, relative to the mill discharge-water, can be considered to result from reactions between the tailings solids and the pore water. From 6- to 10-m depth, the pore-water composition is similar to the mill discharge-water. Pore-water concentration profiles are shown in figure 3. Geochemical equilibrium calculations conducted using MINTEQA2 (Allison et al. 1991) indicate that the water in this interval of site 3 approaches or attains saturation with respect to calcite and siderite, and is undersaturated with respect to dolomite (fig. 4). Mineralogical analyses confirm the presence of calcite, dolomite, and siderite in the tailings solids. The pore water in this interval is consistently undersaturated with respect to jarosite, natrojarosite, and hydronium jarosite, thus indicating that if these phases are present, conditions are favorable for their dissolution. None of these jarosite-group minerals have been detected within this interval. The pore water in this zone is supersaturated with respect to ferric hydroxide ($Fe(OH)_3$), goethite (α-$FeO(OH)$), lepidocrocite (γ-$FeO(OH)$), and akaganeite (β-$FeO(OH,Cl)$). The pore water from surface to the base of the tailings is saturated with respect to gypsum. Gypsum has been detected by X-ray diffraction throughout most of this interval (Jambor et al. 1993).

The pore water from 3- to 9-m at site 1 also reflects the mill discharge-water composition. Most metals in this zone are below detection limits (fig. 3). Geochemical calculations indicate that the pore water below 3-m is slightly supersaturated with respect to calcite, is saturated with respect to dolomite, and one sample indicates saturation with respect to siderite. In the one sample with a significant iron concentration, the pore water is undersaturated with respect to jarosite, natrojarosite, and hydronium jarosite, and is supersaturated with respect to the ferric oxyhydroxide minerals (fig. 4). The pore water throughout the tailings at site 1 is saturated with respect to gypsum, and gypsum has been detected by X-ray diffraction throughout the core-sampled interval (0- to 1.65-m). The similarity between the deep pore water and the current mill discharge-water at sites 1 and 3 indicates that the water in this deep interval has been relatively unreactive with the tailings solids.

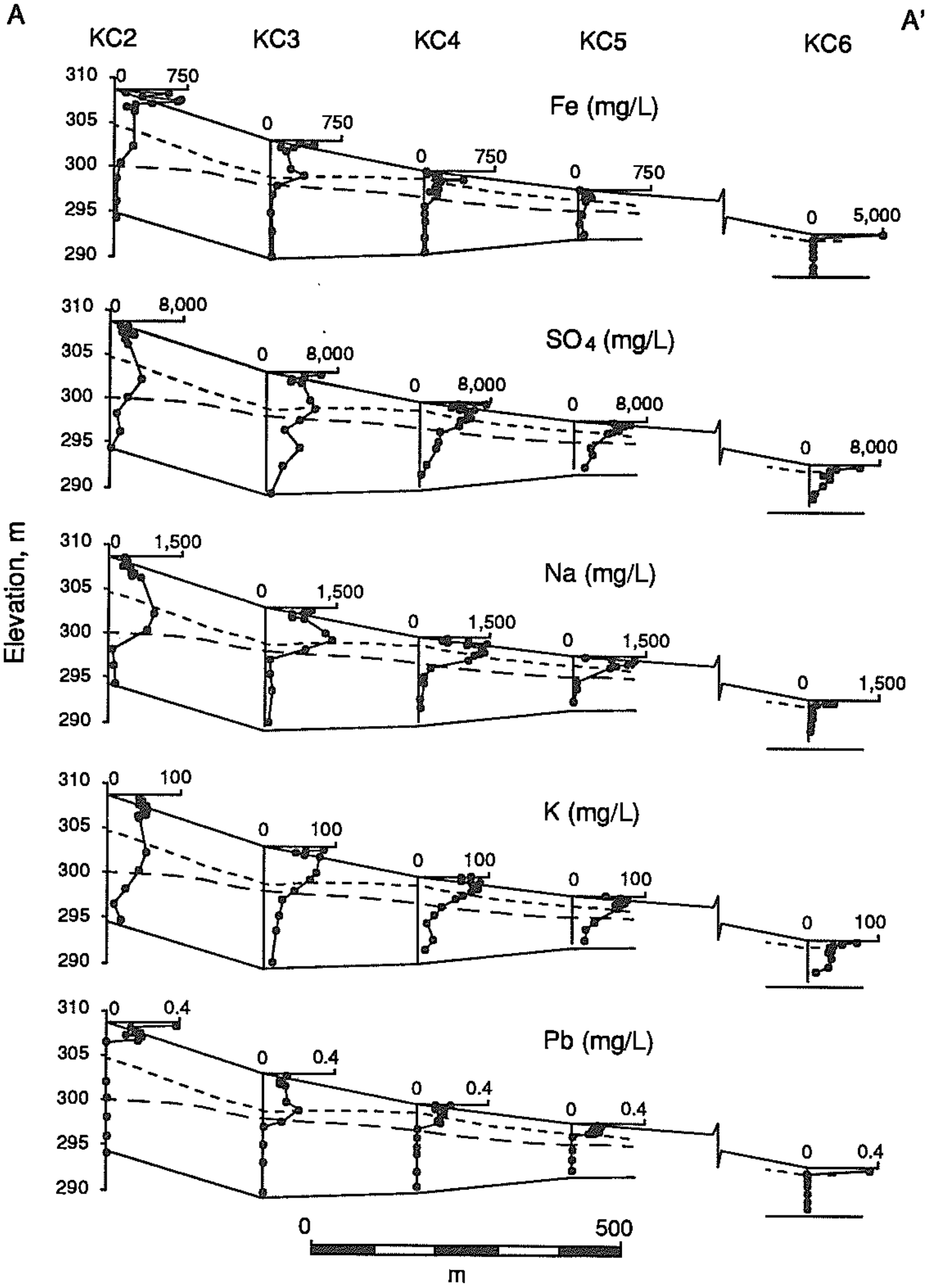

Figure 2. Cross section of pore-water concentration profiles.

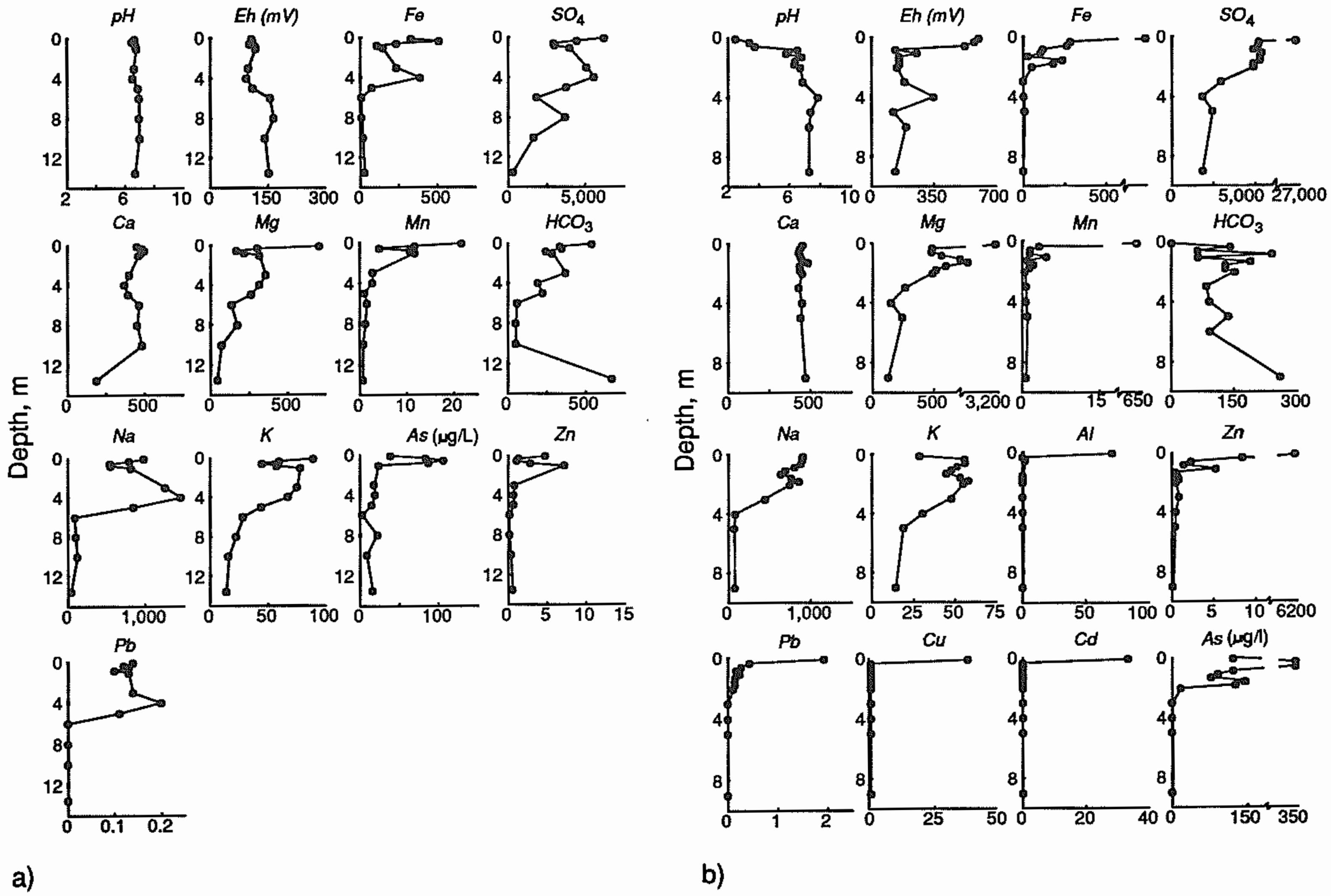

Figure 3. Pore-water concentration profiles for a) site 3 and b) site 1. All concentrations are in mg/L unless shown otherwise.

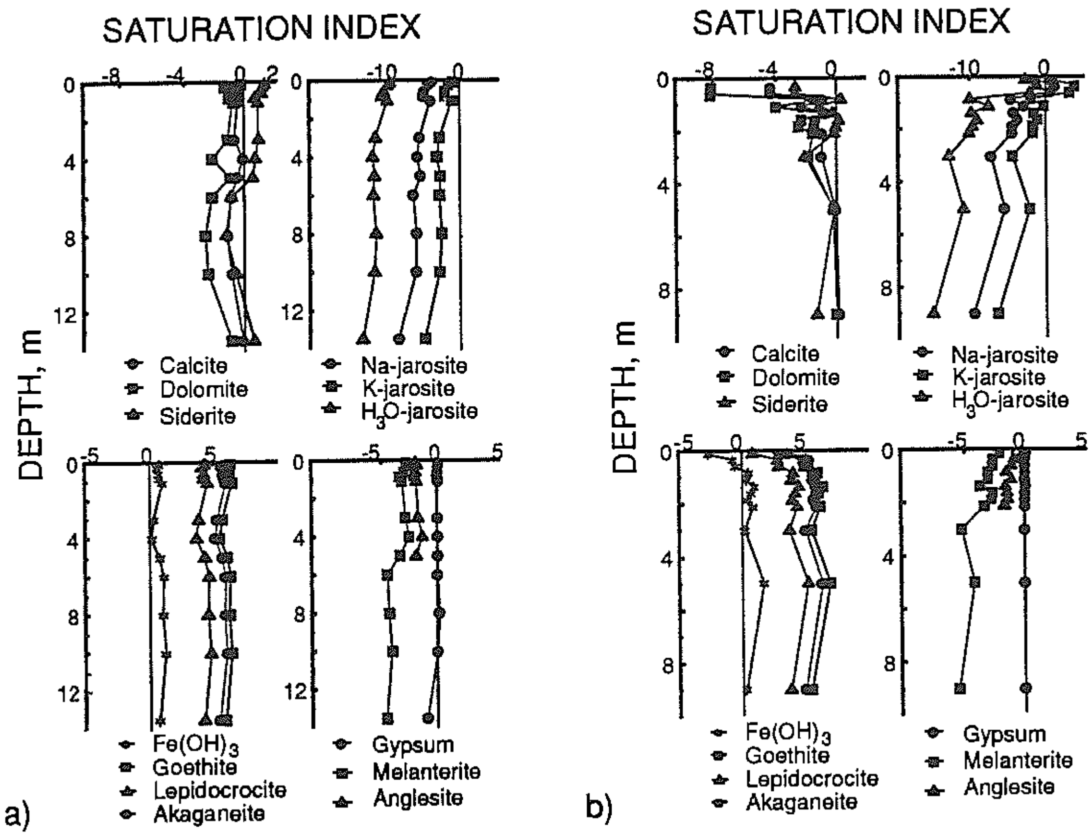

Figure 4. Saturation-index profiles for a) site 3, and b) site 1, calculated with MINTEQA2.

Natrojarosite Disposal Zone

The concentrations of Na, K, Fe, Pb, Zn, As, and SO_4 increase above 6-m depth at site 3 (fig. 3). Sodium, K and H_3O are the principal components in the monovalent cation site of the natrojarosite produced at Kidd Creek (table 2), and the high concentrations of Na and K at this depth interval are best explained by the dissolution of natrojarosite. Tailings pore water above 6-m depth has Na/K = 10 to 20, similar to the average Na/K ratio of 23.7 in natrojarosite from the jarosite pond (Jambor and Owens 1992). Similarly, the increased concentrations of Fe, SO_4, and Pb can be attributed to natrojarosite dissolution. The higher As concentrations in the pore water at this depth also may have resulted from natrojarosite dissolution, as minor solid-solution incorporation of As is documented in jarosite (Dutrizac and Dinardo 1983, Dutrizac and Jambor 1987). Increased concentrations of Zn may be attributed to retention of $ZnSO_4$ in the aqueous phase during co-disposal (Jambor and Owens 1992). Most other metals in this interval remain at or below their detection limits. Increased alkalinity can also be attributed to the dissolution of natrojarosite (reactions 1 and 2.).

$$[Na_{0.75}K_{0.01}(H_3O)_{0.24}]Fe_3(SO_4)_2(OH)_6 + 3H_2O \rightarrow$$
$$3/4Na^+ + 1/100K^+ + 24/100H_3O^+ + 2SO_4^{2-} + 3Fe(OH)_3 + 3H^+ \qquad (1)$$

$$H^+ + (Ca,Mg,Fe,Mn)CO_3 \rightarrow HCO_3^- + (Ca,Mg,Fe,Mn)^{2+} \qquad (2)$$

Above 6-m depth, the decrease of pH (fig. 3) may be a result of natrojarosite dissolution and ferric iron hydrolysis (reaction 1). In the tailings impoundment, the dominant redox-sensitive species are Fe^{2+} and Fe^{3+}. The decrease in

Table 2. Analyses of natrojarosite residue (Jambor and Owens 1992).

	Range, wt %		Mean	σ	Mineralogical Site
	Min	Max	wt %		
Na	1.91	2.97	2.37	0.25	Natrojarosite.
K	0.06	0.16	0.10	0.03	Natrojarosite.
Ca	0.07	0.30	0.15	0.05	Gypsum.
Mg	0.05	0.11	0.08	0.02	Mg sulfate.
Zn	3.93	8.04	6.69	1.21	Zn ferrite, natrojarosite, Zn sulfate.
Cd	0.03	0.08	0.05	0.01	Zn ferrite.
Pb	0.72	2.97	1.63	0.54	Plumbojarosite, anglesite.
Cu	0.12	0.49	0.34	0.09	Covellite, Cu sulfate.
Fe	25.30	31.80	28.53	1.65	Natrojarosite, Zn ferrite.
S	8.58	24.60	12.36	4.82	S°.
As	0.08	0.32	0.16	0.06	Natrojarosite.
SO_4	25.22	31.41	27.77	1.83	Natrojarosite, various sulfate salts.
H_2O	26.06	36.82	32.00	2.97	
In[1]	370	1242	728	210	Natrojarosite.
Ag[1]	151	511	308	90	Natrojarosite, Ag sulfate.

[1] Concentration in grams per kilogram

Notes. - n = 17

- Small amounts of Mn, Sn, Al, and SiO_2 occur in the residue and are derived from MnO_2 and Mn-sulfate, cassiterite, natrojarosite, "silica gel", and quartz, respectively.
- Silica gel is the amorphous hydrated-alumina-silica product of acid leached chlorite.

E_H may be caused by increased activities of Fe^{2+} that result from natrojarosite dissolution followed by the oxidation of pyrite:

$$14[Na_{0.75}K_{0.01}(H_3O)_{0.24}]Fe_3(SO_4)_2(OH)_6 + 3FeS_2 \rightarrow$$
$$21/2Na^+ + 7/50K^+ + 84/25H_3O^+ + 34SO_4^{2-} + 45Fe^{2+} + 36(OH)^- + 24H_2O \qquad (3)$$

Calculated saturation indices (SI) in this zone indicate undersaturation with respect to calcite and dolomite, and slight supersaturation with respect to siderite (fig. 4). These conditions are consistent with the inference of Morin et al. (1988) that precipitation of siderite occurred as a consequence of calcite dissolution in an aquifer affected by acidic Fe- and SO_4-rich tailings drainage water near Elliot Lake, ON. Calculated SI also indicate that the pore water is undersaturated with respect to jarosite, natrojarosite, and hydronium jarosite, suggesting a tendency for the natrojarosite to dissolve, with reaction 1 or 3 favored. This water is supersaturated with respect to goethite, lepidocrocite, and akaganeite, and is very close to saturation with respect to $Fe(OH)_3$. Goethite was the only ferric oxyhydroxide mineral detected by Jambor et al. (1993).

At site 1, a similar zone of high concentrations of Na, K, Fe, Pb, Zn, As, and SO_4 occurs above 3-m depth. As at site 3, the mechanism most likely to be responsible for the increased concentrations in this zone is dissolution of natrojarosite. Increased concentrations of Zn are probably due to adsorbed or aqueous-phase Zn within the natrojarosite residue. Within this interval, Cu, Ni, Co, Cd, Se, Cr, Ag, Ba, Al, NO_3 and PO_4 remain at or below their respective detection limits. Calculations for the interval from 0.6- to 3-m depth at site 1 indicate that the pore water is undersaturated with respect to calcite and dolomite (fig. 4). Undersaturation with respect to siderite occurs from 0.6- to 1.0-m, and saturation to slight supersaturation occurs from 1.0- to 3.0-m. Between 0.6- and 3-m in depth, the pore water is undersaturated with respect to all jarosite phases, is saturated with respect to $Fe(OH)_3$, and is supersaturated with respect to other ferric oxyhydroxides. The zones of increased Na, K, Fe, Pb, Zn, As, and SO_4 concentrations above 6-m depth at site 3 and above 3-m depth at site 1 are characteristic of similar zones at all sites where natrojarosite has been added to the tailings. The pore water affected by natrojarosite occurs below the depth of natrojarosite occurrence (short dashed line, figure 2) as a result of solute transport with the advecting groundwater.

Sulfide Oxidation Zone

High concentrations of SO_4 and metals not associated with natrojarosite occur in the pore water of the upper 0.2-m at site 3. Sulfide oxidation (reaction 4) near the tailings surface is the most likely mechanism for these

$$FeS_2 + 15/4O_2 + 7/2H_2O \rightarrow Fe(OH)_3 + 2SO_4^{2-} + 4H^+ \qquad (4)$$

observed increases. Sulfate is released directly to the pore water by sulfide oxidation. Sulfide oxidation generates H^+ ions, which are neutralized by carbonate-mineral dissolution (reaction 2). These reactions contribute Ca, Mg, Fe, Mn, and HCO_3 to the pore water. MINTEQA2 calculations indicate supersaturation with respect to siderite, and undersaturation with respect to calcite and dolomite in the top 0.2-m at site 3. These calculations support the inferred mechanism for increased Mn, Mg, and alkalinity in the pore water at this depth: up to 5.2 wt % Mn occurs in solid solution within siderite, dolomite, and ankerite, and up to 9.7 wt % Mg occurs in solid solution with these minerals (Jambor et al. 1993). The tailings water within this interval is undersaturated with respect to jarosite, natrojarosite, and hydronium jarosite, indicating that conditions are favorable for the dissolution of these minerals. The pore water is saturated with respect to $Fe(OH)_3$ and gypsum, and is supersaturated with respect to goethite, lepidocrocite, and akaganeite, suggesting that $Fe(OH)_3$ and gypsum may control the pore-water concentrations of Fe and Ca through precipitation-dissolution processes.

The pore water from the surface to 0.6-m depth at site 1 contains high concentrations of metals and SO_4 (fig. 3), reflecting the effects of sulfide oxidation: the H^+ released by pyrite oxidation (reaction 4) has decreased the pore-water pH to between 2.5 and 4, and the E_H has increased to between 525- and 600-mV because of the increased solubility of Fe^{3+} at low pH. Sulfide oxidation near the surface releases H^+ ions, which are neutralized by carbonate-mineral dissolution, causing increases in the concentrations of Ca, Mg, Fe, and Mn. The high concentrations of Mg and Mn (fig. 3) suggest that dissolution of dolomite is occurring. Also released by sulfide oxidation are Fe, Zn, Pb, Cu, Ni, Co, and Cd, which are relatively soluble under low pH conditions. Where the pH decreases below 5, Al concentrations increase, probably because of pH buffering reactions involving dissolution of aluminum-silicate minerals such as chlorite, muscovite, and albite. The alkalinity of the pore water decreases from 52 to 0 mg/L HCO_3 between 0.6-m depth and the surface, suggesting either depletion of the carbonate-mineral acid-neutralization capacity, or that the rate of carbonate-mineral dissolution is too slow to maintain measurable alkalinity concentrations. Mineralogical study indicates the latter since dolomite and siderite are present in this interval. The high concentrations of Cd, Co, Cu, Ni, Cr, and Al in the pore water distinguishes the effects of sulfide oxidation from the effects of natrojarosite dissolution. Geochemical modeling for the zone 0- to 0.6-m at site 1 indicates that the pore water is undersaturated with respect to all of the carbonate minerals (fig. 4). The pore water is saturated to supersaturated with respect to jarosite, is saturated with respect to natrojarosite, and is undersaturated with respect to hydronium jarosite. The SI of the ferric hydroxide and oxyhydroxide phases decrease in this interval. The pore water also approaches saturation with respect to anglesite ($PbSO_4$) in the upper 0.2-m, suggesting a possible control on the near-surface pore-water Pb concentrations.

Comparison with Mill Discharge-Water Chemistry

The geochemical data from site 1 and site 3, normalized to their respective concentrations in the mill discharge-water, show changes in pore-water composition that have occurred since the tailings were deposited (fig. 5). Below the natrojarosite disposal zone there are slight increases of Mg, Na, Fe, and SO_4 relative to the discharge water, but except for Fe, these differences could be a result of variation in the discharge-water composition. The pore water in the zones affected by natrojarosite disposal displays similar patterns at sites 1 and 3. Concentrations of Na, K, Fe, Zn, Pb, Mn, As, and SO_4 are sharply increased relative to the discharge water. The concentrations of metals are highest at the surface where tailings have been affected by sulfide oxidation. Sulfide oxidation is associated with increased concentrations of Mg, Fe, Zn, Pb, Cu, Ni, Co, Cd, Mn, As, Cr, Al, and SO_4.

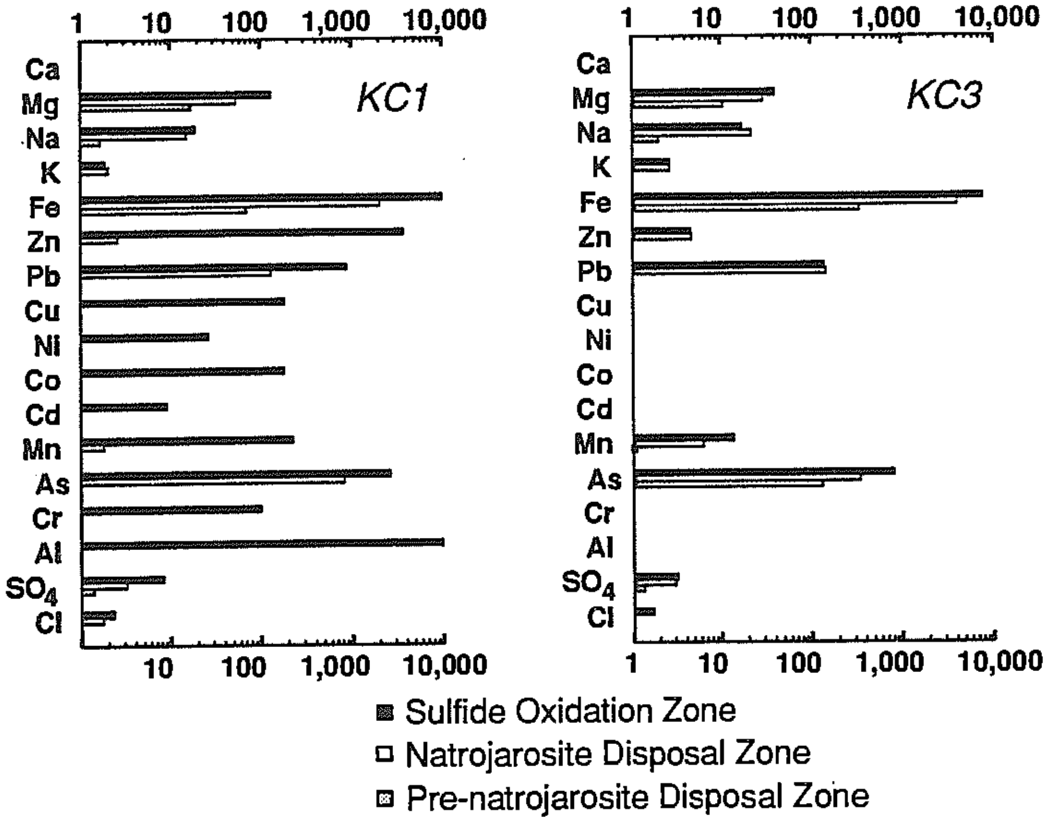

Figure 5. Average concentrations from the zones affected by sulfide oxidation and by natrojarosite dissolution, and the deep, pre-natrojarosite zone, all normalized to the average mill discharge-water concentrations from table 1.

Conclusions

The data define three geochemical zones, the deepest zone displaying pore-water concentrations of metals and sulfate similar to the present mill discharge-water concentrations. Intermediate depths display elevated concentrations of Na, K, Fe, Mg, Mn, Pb, Zn, As, HCO_3, and SO_4 relative to the present mill discharge-water. These increases are a result of the dissolution of natrojarosite that has been co-disposed with the tailings since 1985. Mineralogical studies indicate that a significant mass of natrojarosite remains in the tailings. Pore water near the surface contains high concentrations of Mg, Mn, Fe, Zn, Pb, Cu, Ni, Co, Cd, As, Cr, Al, and SO_4 that are the result of sulfide oxidation near the tailings surface, causing the release of metals and sulfate to the pore water. Both sulfide oxidation and natrojarosite dissolution cause the dissolution of carbonate minerals, consuming the acid-neutralization capacity of the tailings. Acidity is contributed to the pore water through increased pore-water Fe^{2+} concentrations related to related to natrojarosite dissolution and sulfide oxidation.

Acknowledgements

Funding for this study was provided by Falconbridge Limited, Kidd Creek Division and by the Mine Environment Neutral Drainage (MEND) program of Ontario. We would like to thank Falconbridge Limited, particularly G. Marrs and J.D. Scott, for their help and cooperation in publishing this work.

Literature Cited

Allison, J. D., D. S. Brown and K. J. Novo-Gradac. 1991. MINTEQA2/PRODEFA2, A geochemical assessment model for environmental systems: version 3.0 user's manual. U.S. Environmental Protection Agency Report 600/3-91/021

Dutrizac, J. E. and O. Dinardo. 1983. The co-precipitation of copper and zinc with lead jarosite. Hydrometallurgy 11:61-78. http://dx.doi.org/10.1016/0304-386X(83)90016-6

Dutrizac, J. E. and J. L. Jambor. 1987. The behaviour of arsenic during jarosite precipitation: arsenic precipitation at 97 °C from sulphate or chloride media. Canadian Metallurgical Quarterly 26:91-101. http://dx.doi.org/10.1179/cmq.1987.26.2.91

Garrels, R. M. 1960. Mineral equilibria at low temperature and pressure. Harper and Brothers, 254 pp.

Jambor, J. L. and D. R. Owens. 1992. Mineralogical characterization of process products and secondary phases in the Kidd Creek jarosite impoundment, Timmins, Ontario. CANMET Division Report, MSL 92-29 (CR).

Jambor, J. L., D. R. Owens, P. Carrière and R. Lastra. 1993. Mineralogical investigation of tailings and associated waste products, and the distribution of natrojarosite in the Kidd Creek main tailings cone, Timmins, Ontario. CANMET Division Report, MSL 93-20 (CR).

Morin, K. A., J. A. Cherry, N. K. Dave, T. P. Lim and A. J. Vivyurka. 1988. Migration of acidic groundwater seepage from uranium tailings impoundments, 1. Field study and conceptual hydrogeochemical model. Journal of Contaminant Hydrology 2:271-303. http://dx.doi.org/10.1016/0169-7722(88)90008-3

Robinsky, E., S. L. Barbour, G. W. Wilson, D. Bordin and D. G. Fredlund. 1991. Thickened sloped tailings disposal - an evaluation of seepage and abatement of acid drainage. *In* Second International Conference on the Abatement of Acidic Drainage, Vol. 1 pp. 529-550.

Scott, J. D. and U. Dienstbach. 1990. Circuit optimization, with silver recovery options and deportment, in the Kidd Creek zinc plant. *In* Lead-Zinc '90, *edited by* T.S. Mackey and R.D. Prengaman. The Minerals, Metals and Materials Society, Warrendale, Pennsylvania, pp. 121-134.

Walker, G. W. and G. W. Mannard. 1974. Geology of the Kidd Creek mine, a progress report. Canadian Institute of Mining and Metallurgy Bulletin 67:41-57.